Chapter 3 Results

3.1 *V. alginolyticus pepD* Gene Sequence

The putative aminoacylhistidine dipeptidase-encoding gene, *pepD*, has been isolated from *V. alginolyticus* ATCC 17749 genome. The *V. alginolyticus pepD* gene contained 1473 nucleotides, which encodes a protein of 490 amino acids with a calculated molecular mass of 53.6 kDa and a theoretical isoelectric point (p*I*) of 4.70 (Fig. 8).

The protein-protein BLAST (blastp) search indicated that the amino acid sequence deduced from *V. alginolyticus pepD* gene was similar to that of aminoacylhistidine dipeptidase of *Vibrio* spp. and other bacteria (Appendix 3). All sequences listed in the Appendix 3, however, only *E. coli* PepD had been characterized biochemically. Further analysis of *V. alginolyticus* PepD sequence reveals that 7 amino acids might be involved in the active site of PepD, which five of them are the metal-binding residues and two are catalytic residues (It will be discussed more detailedly at 3.7) (Fig. 8). Moreover, six proteins, *A. proteolytica* aminopeptidase (AAP) (Chevrier *et al.*, 1994), *Streptomyces griseus* aminopeptidase S (Greenblatt *et al.*, 1997) (SGAP), *Pseudomonas sp.* carboxypeptidase G2 (CPG2) (Rowsell *et al.*, 1997), *L. delbrueckii* peptidase V (PepV) (Jozic *et al.*, 2002), *N. meningitidis* succinyl diaminopimelate desuccinylase (DapE) (Badger *et al.*, 2005), and *Salmonella typhimurium* peptidase T (Hakansson and Miller, 2002), the members of peptidase clan MH with the structures solved, were aligned with *V. alginolyticus* PepD on their amino acid sequences (Table 7). However, PepD shows all strikingly low identities to these proteins.

The nucleotide sequence data of *V. alginolyticus pepD* reported in this thesis has deposited in the GenBank nucleotide sequence database with the accession number DQ335448.

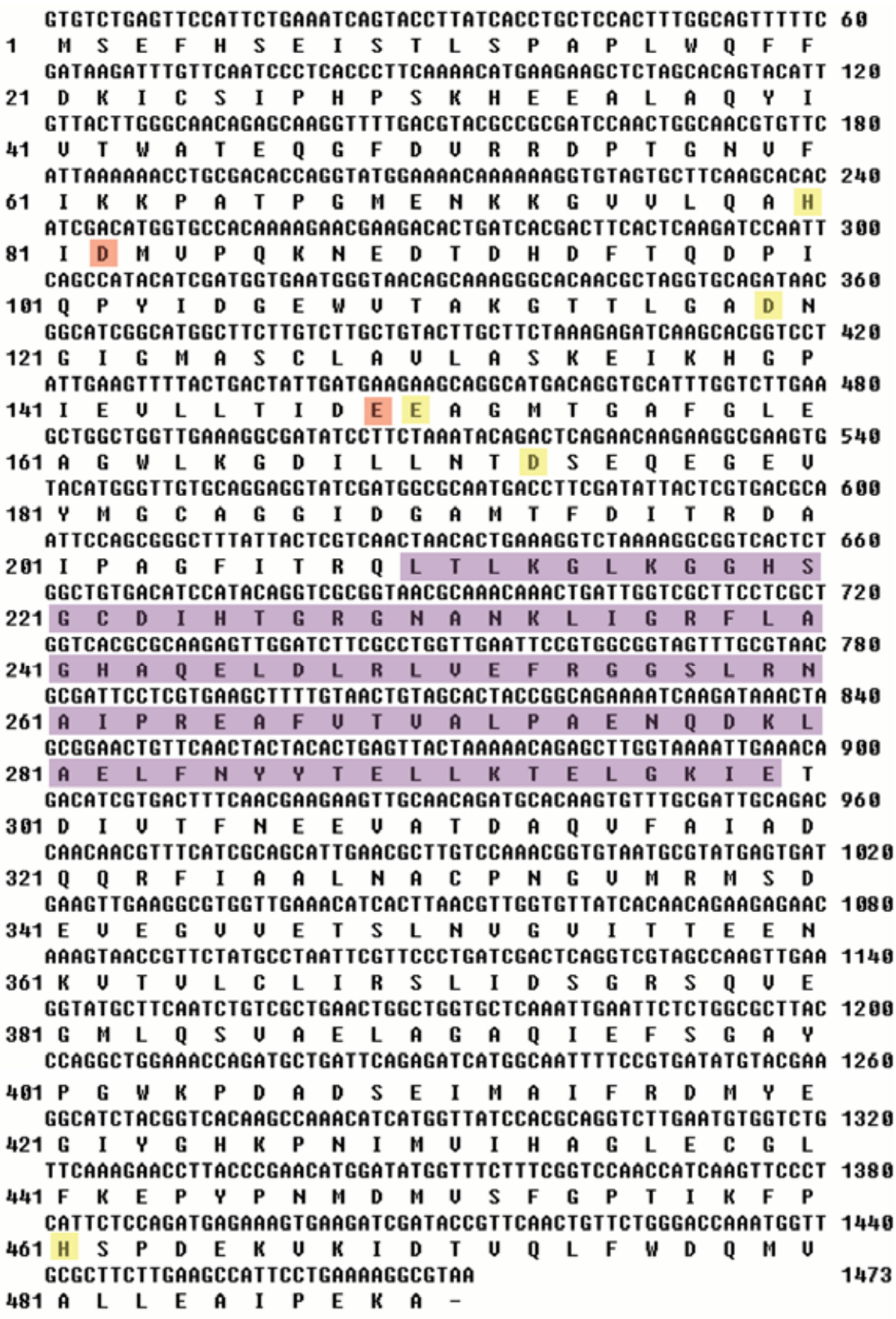

Fig. 8. Nucleotide sequences and predicted amino acid sequences of *V. alginolyticus pepD* gene. His80, Asp119, Glu150, Asp173, and His461 showed in yellow color are expected metal ion binding residues. Asp82 and Glu149 showed in pink color are putative catalytic residues. Leu210-Glu299 showed in purple color is expected a dimerization domain which is predicted by Pfam (http://pfam.cgb.ki.se).

Table 7. Homology analysis between *V. alginolyticus* PepD and proteins of peptidase clan MH

Species	Name	Length (a.a.[c])	Identity (%)
A. proteolytica[a]	Aminopeptidase (AAP)[b]	291	6
S. griseus	Aminopeptidase S (SGAP)	284	8
Pseudomonas sp.	Carboxypeptidase G2 (CPG2)	393	12
L. delbrueckii	Peptidase V (PepV)	470	9
N. meningitidis	Succinyl diaminopimelate desuccinylase (DapE)	387	10
S. typhimurium	Peptidase T (PepT)	411	10

[a] *Aeromonas proteolytica* is renamed as *Vibrio proteolytica* now.
[b] The common abbreviation of the protein is shown in parentheses.
[c] a.a. = amino acid.

3.2 Expression and Purification of *V. alginolyticus* PepD in *E. coli*

V. alginolyticus pepD was ligated into pET-28(+) vector and expressed in *E. coli* BL21(DE3)pLysS. *E. coli* BL21(DE3)pLysS harboring pET-28a(+)-pepD was cultured in LB medium supplemented with kanamycin and 0.5 M IPTG for 16 hrs at 37℃ to express tremendous amounts of soluble PepD in *E. coli* cytoplasm. Expressed PepD with a Hig-tag on the *N*-terminus was purified by Ni-NTA column chromatography. The Ni-NTA resin-bound PepD would be washed out by 20 mM Tris-HCl, 0.5 M NaCl, pH 7.4 buffer containing 100 mM imidazole with high purity. The purified fractions were collected and dialyzed with 50 mM Tris-HCl, pH 7.4 at 4℃ to remove the remaining salts. The dialyzed sample performed on SDS-PAGE finally gives a single band with molecular mass of ~55 kDa (Fig. 9), which closely meet the calculated molecular mass of *V. alginolyticus* PepD.

The purified fraction was further characterized with the activity assay on L-carnosine (β-Ala-L-His) hydrolysis test. The expressed PepD could catalyze the hydrolysis of

L-carnosine to β-alanine and L-histidine under standard conditions as described on 2.9.1. The purified enzyme was also performed on SDS-PAGE and submitted to internal amino acid sequencing, and the result confirms that the purified enzyme was *V. alginolyticus* PepD.

For future experimental demand, the purified PepD with L-carnosine hydrolyzing activity was immunized mice to produce anti-PepD mAbs as described on Appendix 4. The western blot carried out with anti-PepD mAb showed a single band on the film (Fig. 9). This result indicates that the PepD antibody could specifically recognize the expressed *V. alginolyticus* PepD. Seven hybridoma clones, pepD-1-6G, pepD-1-8A, pepD-2-12F, pepD-3-1D, pepD-3-1E-5F, pepD-3-1G, and pepD-3-2A, were found to recognize *V. alginolyticus* PepD.

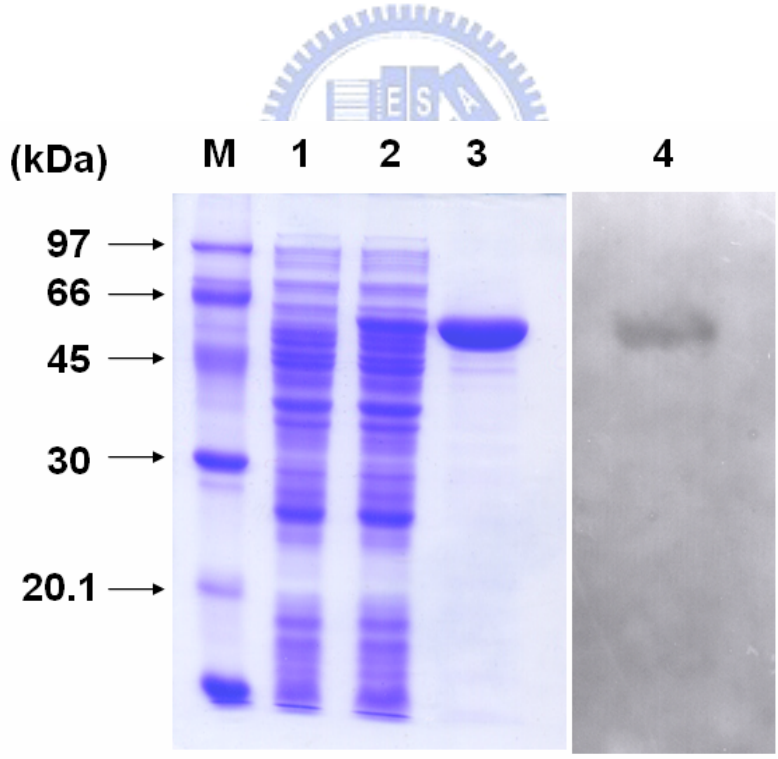

Fig. 9. SDS-PAGE and western blot analysis of purified PepD. *Lane M*, LMW protein marker. *Lane 1*, cell crude extracts of *E. coli* BL21(DE3)pLysS carrying pET-28a(+). *Lane 2*, cell crude extracts of *E. coli* BL21(DE3)pLysS carrying pET-28a(+)-pepD. *Lane 3*, purified PepD from the Ni-NTA column. *Lane 4*, western blot analysis of purified PepD using PepD antibody.

3.3 Effects of pH and Temperature on Activity of PepD

To examine the effect of pH on PepD activity, two buffer systems with overlapping pH ranges were used (Fig. 10). The rate of hydrolysis of the substrate L-carnosine at 37℃ for 60 min reached its maximum value at pH 7.0-7.4 and dropped at more acidic and alkaline pH, retaining only 80% and 86% of its maximal activity at pH 6 and pH 8.5, respectively.

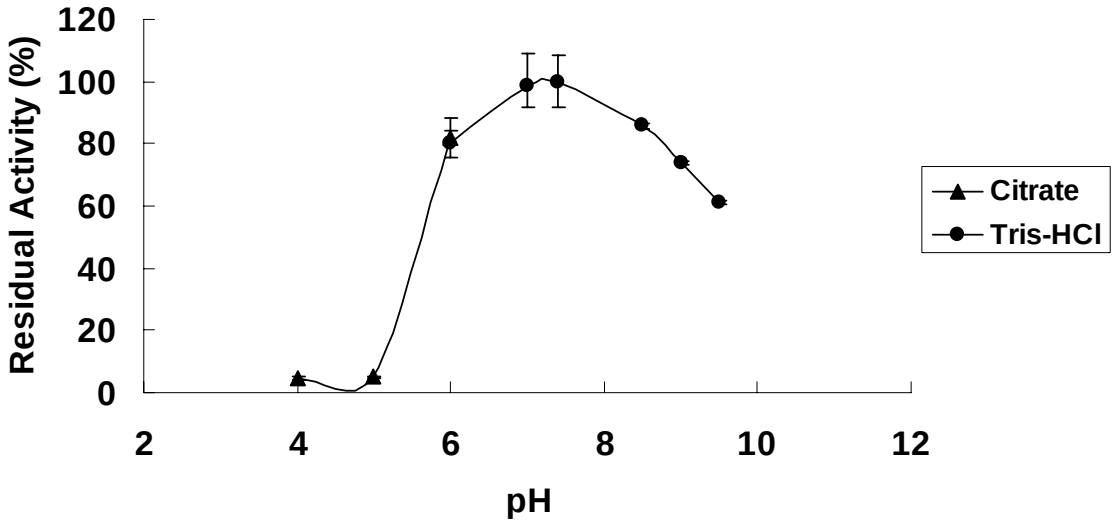

Fig. 10. pH optimum of PepD. The assays were performed as described on 2.9.2, which two buffer systems citrate (pH 4, 5, and 6) and Tris-HCl (pH 6, 7, 7.4, 8.5, 9, and 9.5) were used. The activity at pH 7.4 was defined as 100%.

The effect of temperature on *V. alginolyticus* PepD activity was also examined at various temperatures between 4 and 70℃. After pre-incubated at different temperatures for 30 min, the remaining PepD activity was assayed under standard conditions. The *V. alginolyticus* PepD remains over 95% of its full activity at 4 to 50℃ and rapidely loses its activity above 50℃ (Fig. 11). The optimal temperature for PepD activity was also investigated between 4 and 70℃. The enzymatic reaction carried out at 37℃ shows the highest activity than that at other temperatures (Fig. 12). Thus, the optimum PepD activity was carried out at pH 7.4 and 37℃.

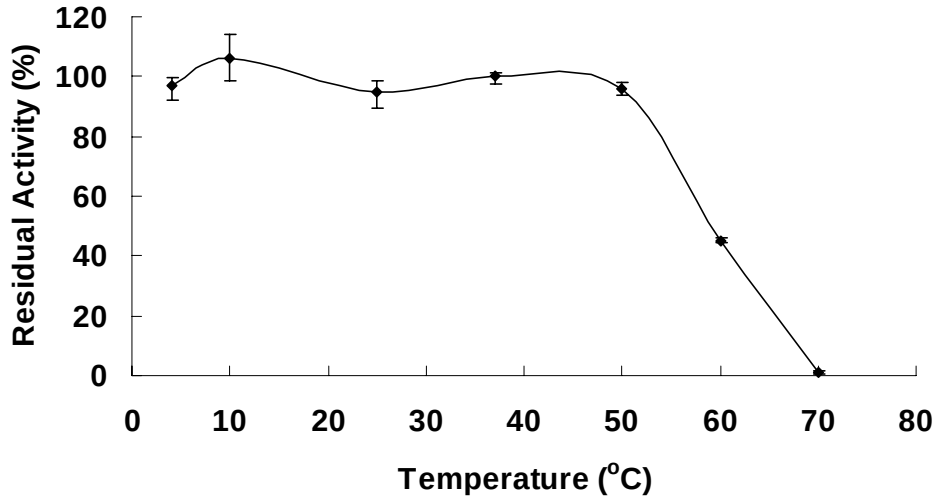

Fig. 11. Thermostability of PepD. The assays were performed as described on 2.9.3 at 4, 10, 25, 37, 50, 60, and 70℃. The activity at 37℃ was defined as 100%.

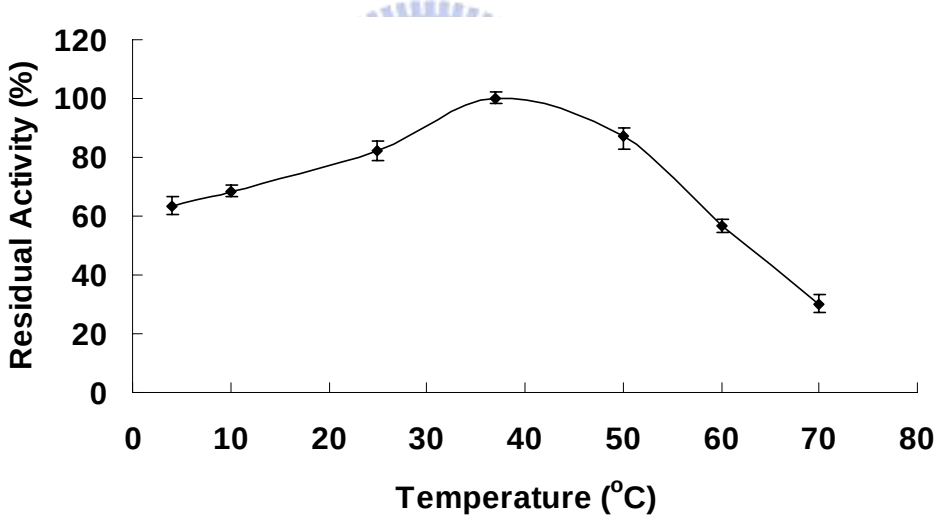

Fig. 12. Temperature optimum of PepD. The enzyme was pre-incubated at 4, 10, 25, 37, 50, 60, and 70℃ for 30 min followed by performing the standard activity assay (see 2.9.1) at 37℃ for 1 hr. The activity at 37℃ was defined as 100%.

3.4 Effects of Inhibitors on Activity of PepD

To classify the catalytic type of *V. alginolyticus* PepD four common peptidase inhibitors were examined on their effects to the PepD activity. The PepD activity was measured under standard conditions after pre-incubated with various concentrations of inhibitors at 37℃ for 30 min. The inhibition test of EDTA was performed initially at the successively diluted concentrations. Because of the rapid loss of PepD activity at the present of 0.02 and 0.01 mM of EDTA, the more subdivided concentrations of EDTA between 0.02 and 0.01 mM were performed. *V. alginolyticus* PepD activity was strongly inhibited by a metal-chelating agent EDTA at a final concentration of 0.02 mM (1.86%) and a peptide analogue inhibitor bestatin at a final concentration of 0.3 mM (5.9%) (Fig. 13). Value in parentheses indicates the relative residual activity. However, benzamidine, a serine endopeptidase inhibitor, and *N*-ethylmaleimide (NEM), a cysteine endopeptidase inhibitor, had no apparent inhibition effect on PepD activity at low centrations. Therefore, *V. alginolyticus* PepD was identified as a metallopeptidase.

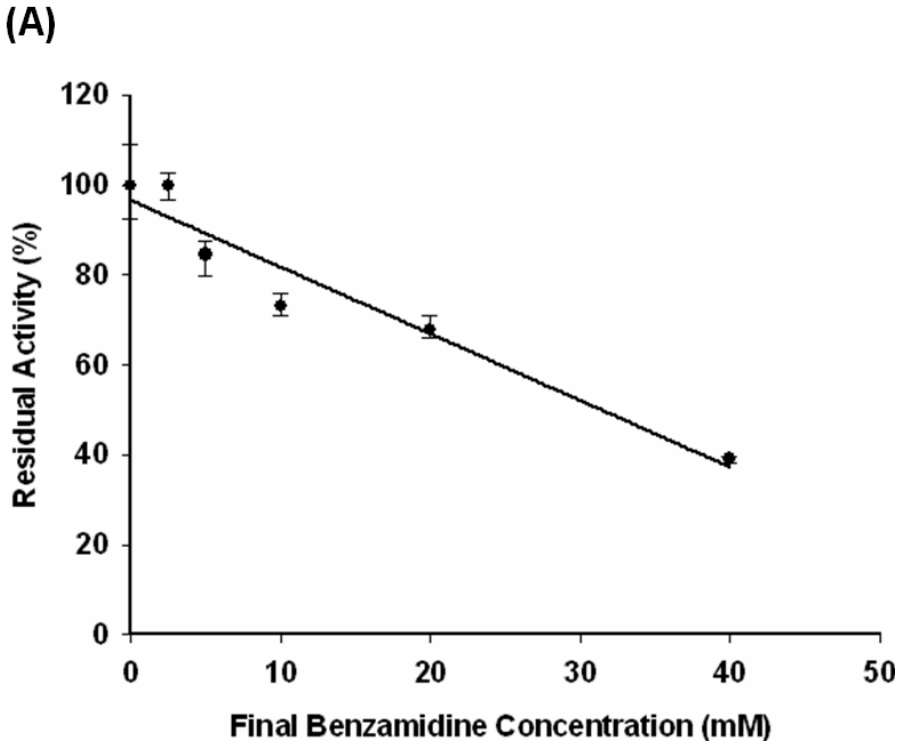

(B)

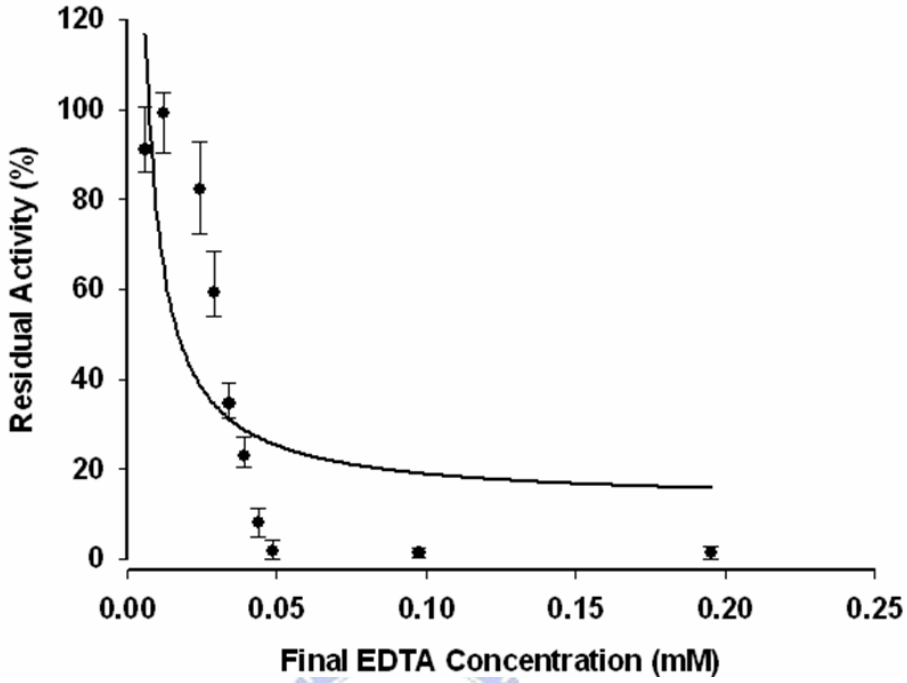
120
100
80
60
40
20
0
Residual Activity (%)
0.00
0.05
0.10
0.15
0.20
0.25
Final EDTA Concentration (mM)

(C)

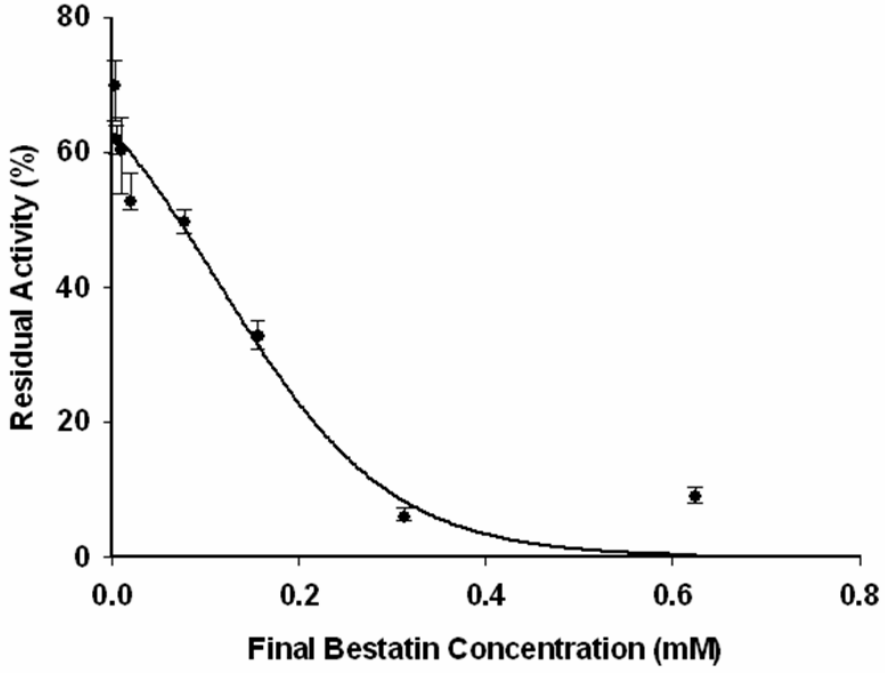
80
60
40
20
0
Residual Activity (%)
0.0
0.2
0.4
0.6
0.8
Final Bestatin Concentration (mM)

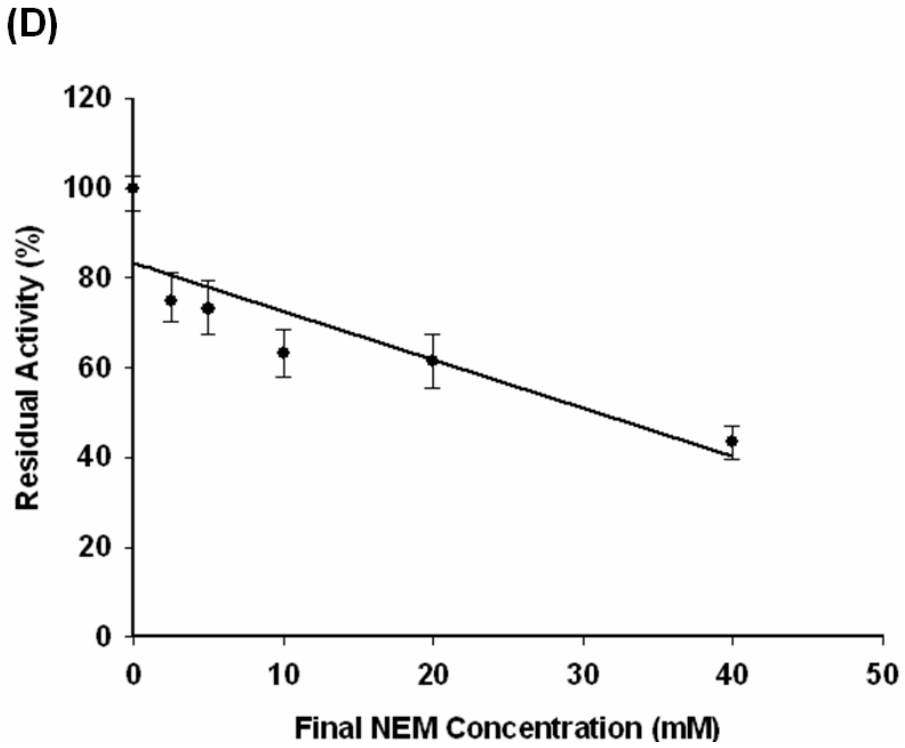

Fig. 13. Effect of peptidase inhibitors on PepD activity. (A) Serine endopeptidase inhibitor benzamidine. (B) Metal-chelating agent EDTA. (C) Peptide analogue inhibitor bestatin. (D) Cysteine endopeptidase inhibitor *N*-ethylmaleimide (NEM). The activity without inhibitor present was defined as 100%.

3.5 Substrate Specificity

The PepD from *E. coli* was identified as a dipeptidase with board substrate specificity (Schroeder *et al.*, 1994). To study the substrate specificity of PepD from *V. alginolyticus* compared with from *E. coli*, the purified enzyme was assayed with 5 Xaa-His dipeptides and 2 histidine-containing tripeptides as described on 2.9.4. The enzyme activity on L-carnosine (β-Ala-L-His), the known substrate of aminoacylhistidine dipeptidase (PepD), was defined as 100%. *V. alginolyticus* PepD hydrolyzes α-Ala-L-His with 1.76 times higher efficiency than β-Ala-L-His which differs only in the position of amino group and digests Gly-His with 82% efficiency of β-Ala-L-His (Fig. 14). The enzyme had no apparent activity on β-Asp-L-His, and the hydrolysis of L-homocarnosine (GABA-His) was under the detection limit. Moreover, tripeptides containing histidine in the central or *C*-terminal position are not degraded, indicating that *V. alginolyticus* PepD is a dipeptidase in activity.

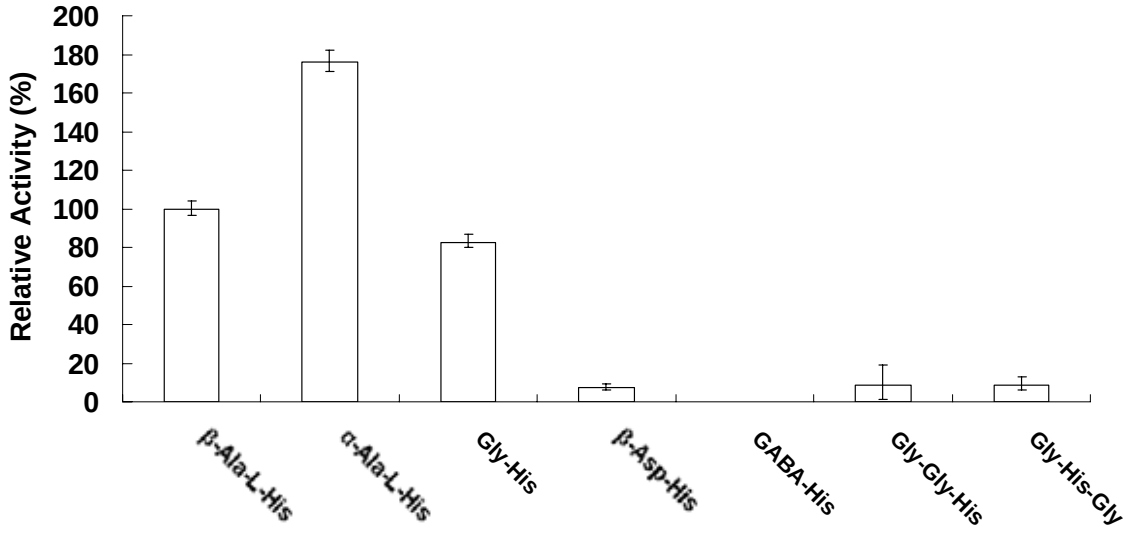

Fig. 14. Substrate specificity of PepD for Xaa-His dipeptides and histidine-containing tripeptides. Purified recombinant PepD proteins were incubated for 1 hr at 37℃ with 5 Xaa-His dipeptides and 2 tripeptides at 1 mM final concentration, and the activity was measured as standard activity assay (see 2.9.1). Values are expressed as relative activity setting the degradation of carnosine to 100%.

3.6 Enzyme Kinetics

The enzyme kinetics of *V. alginolyticus* PepD for L-carnosine was performed as described on 2.9.6. The V_{max} and K_m values of *V. alginolyticus* PepD (10 μg, 0.902 μM) for L-carnosine calculated from the respective Lineweaver-Burk plot were 7.14 μM/min and 5.38 mM, respectively (Fig. 15). Therefore, the turnover number (k_{cat}, $k_{cat} = V_{max}/[E]_T$) of *V. alginolyticus* PepD for L-carnosine in 50 mM Tris-HCl, pH 7.4 at 37℃ is 0.132 s^{-1} and the catalytic efficiency (k_{cat}/K_m) is 2.45×10^{-2} mM^{-1} s^{-1}.

The determined K_m value of PepD was 5.64 mM from *E. coli* (Schroeder *et al.*, 1994) and 0.25 mM from *S. typhimurium* (Kirsh *et al.*, 1978). The other kinetics values including k_{cat}, k_{cat}/K_m, and specific activity of PepD, however, were first identified.

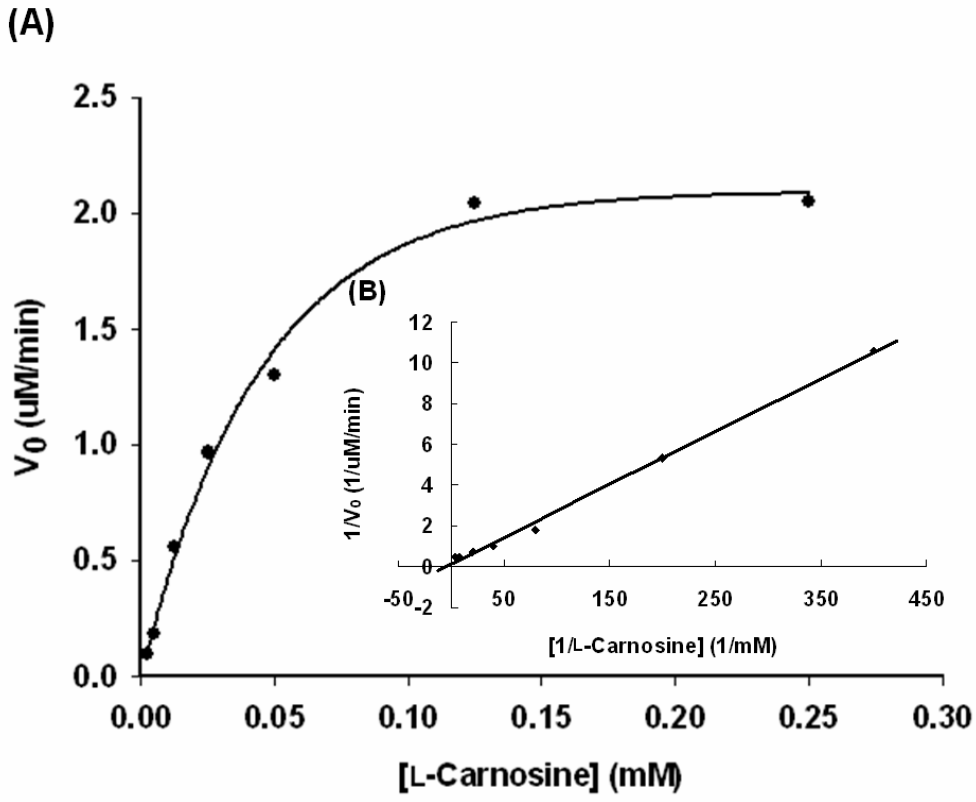

Fig. 15. (A) Michaelis-Menten plot for PepD catalyzed the hydrolysis of L-carnosine in 50 mM Tris-HCl, pH 7.4 at 37℃. (B) Lineweaver-Burk plot calculated from the respective Michaelis-Menten plot.

3.7 Site-directed Mutagenesis Analysis of *V. alginolyticus* PepD

To investigate the essential amino acids for *V. alginolyticus* PepD activity, site-directed mutagenesis analysis on PepD residues were performed. *L. delbrueckii* PepV, the only carnosine-hydrolyzing enzyme with structure being solved, was aligned with *V. alginolyticus* PepD in order to select the potent residues. However, low amino acid sequence indentity between both sequences were observed (Table 7) except for the conserved active site residues of *L. delbrueckii* PepV (Fig. 16). These residues include His80, Asp119, Glu150, Asp173, and His461 expected for metal binding, and Asp82 and Glu149 for catalysis (Fig. 8). The 7 putative active site residues were consequently investigated by alanine scanning mutagenesis.

The pET-28a(+) plasmid ligated with *V. alginolyticus pepD* wild-type gene (pET-pepD-WT) was 6.8 kbp long in length with 1 *Ava*I, 1 *Nco*I, 1 *Nde*I, 1 *Nhe*I, 1 *Not*I, 1 *Pvu*I and the absence of *Sac*II restriction site. The desired mutants generated as described on 2.11 will incorporate an additional restriction site which could be checked by restriction enzymes (Appendix 5-6). The mutant plasmids were checked by DNA sequencing, and expressed in *E. coli* BL21(DE3)pLysS as the same experimental procedure of *V. alginolyticus* wild-type PepD to obtain the mutant PepD proteins.

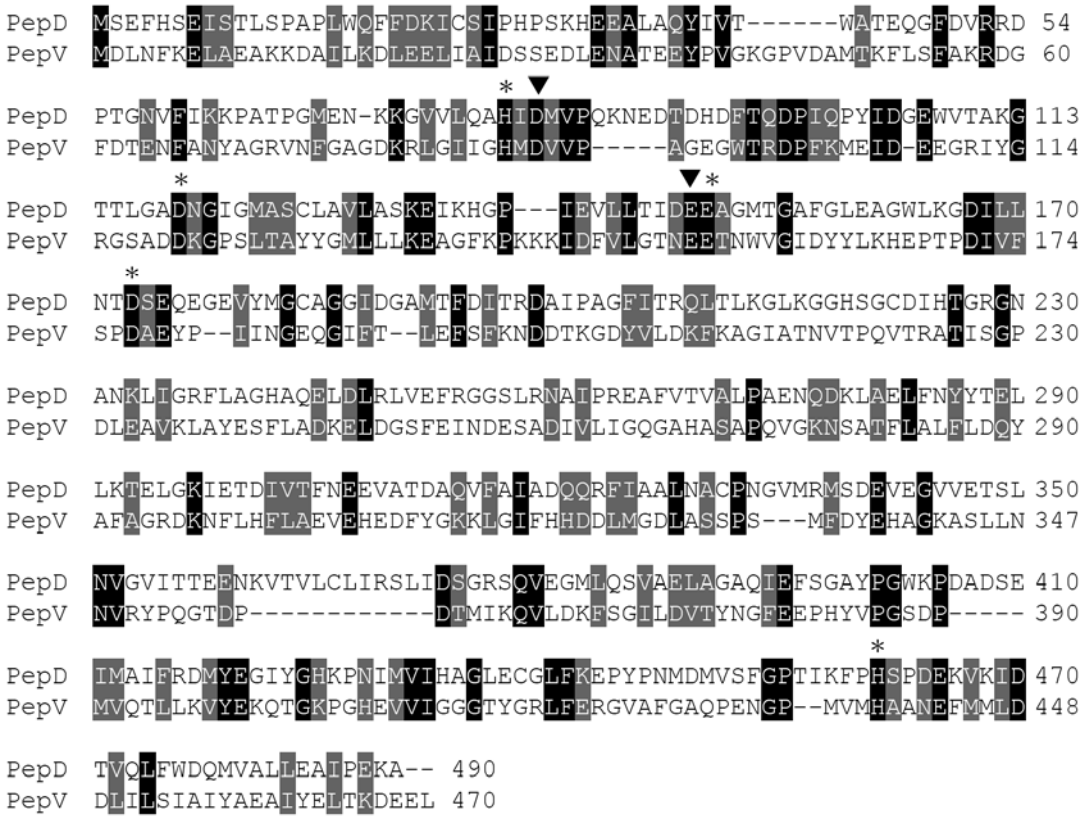

Fig. 16. Comparison of the amino acid sequences of *V. alginolyticus* PepD and *L. delbrueckii* PepV. Identical and conserved amino acids between the sequences are marked in black and gray, respectively. Dashed lines indicate the gaps introduced for better alignment. Proposed active site residues Asp82 and Glu149 in PepD are marked by arrowheads, and proposed metal ion binding residues His80, Asp119, Glu150, Asp173, and His461 are marked by asterisks.

The purified wild-type and mutant PepD proteins gave single bands at the same position with molecular mass of ~55 kDa, indicating the successful expression and purification (Fig. 17). The samples are also performed on Native-PAGE analysis to observe the differences of native form of mutants and wild-type PepD, which is indicated as a homodimer in *E. coli* (Klein *et al.*, 1986). However, through Native-PAGE analysis, only a weak band with molecular mass near 140 kDa of the protein marker was observed (Fig. 18), and so were the PepD mutants. The PepD WT protein likely tends to form a monomer in its native state. Interestingly, the PepD D82A mutant seems to aggregate spontaneously, which differs from other mutants. The reason of this phenomenon might be required for further study.

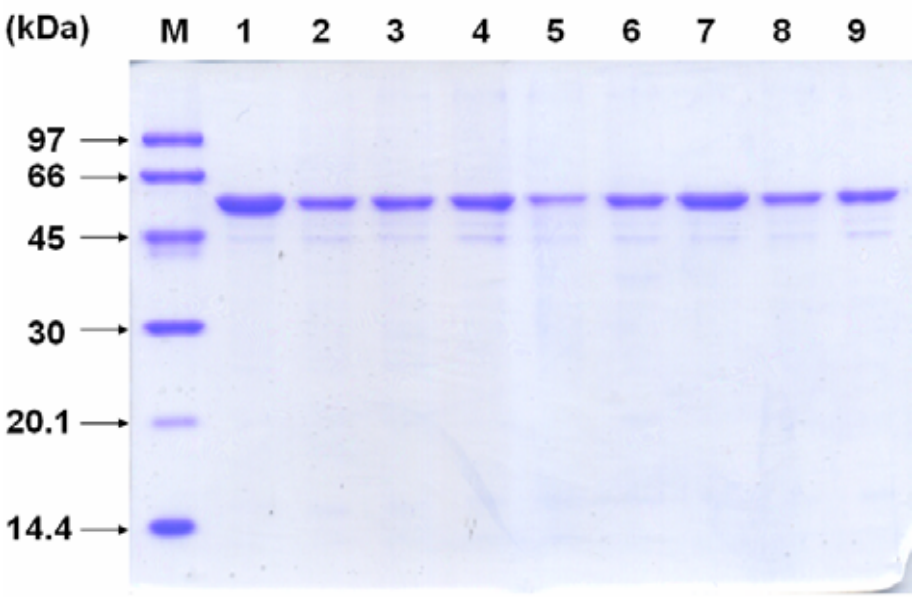

Fig. 17. SDS-PAGE of purified PepD wild-type and mutant proteins. *Lane M*, LMW protein marker. *Lane 1*, PepD wild-type (WT). *Lane 2*, PepD His80A mutant. *Lane 3*, PepD Asp82A mutant. *Lane 4*, PepD Asp119A mutant. *Lane 5*, PepD Glu149A mutant. *Lane 6*, PepD Glu150A mutant. *Lane 7*, PepD Asp173A mutant. *Lane 8*, PepD His461A mutant. *Lane 9*, PepD Asp119AGlu150A mutant.

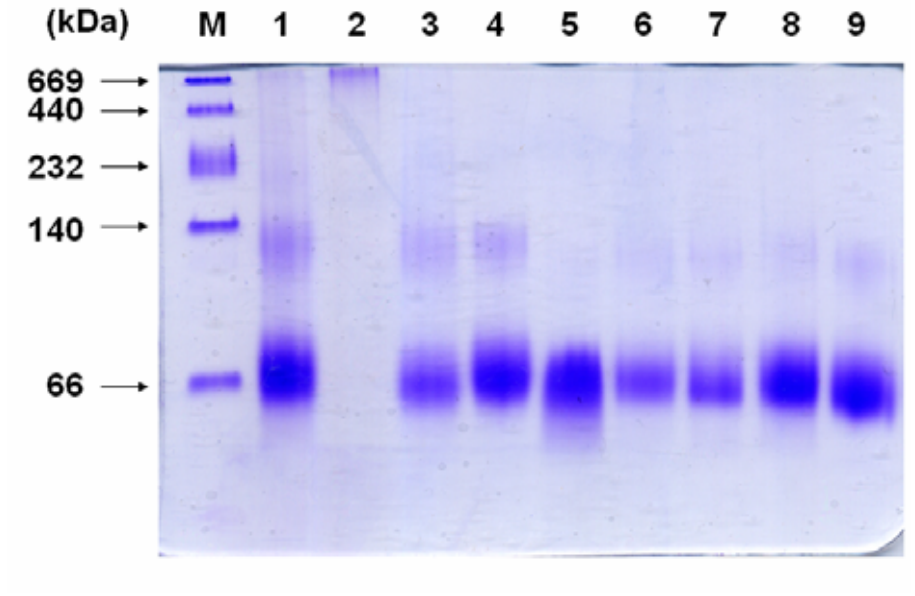

Fig. 18. Native PAGE of purified PepD wild-type and mutant proteins. *Lane M*, HMW Native protein marker. *Lane 1*, PepD WT. *Lane 2*, PepD His80A mutant. *Lane 3*, PepD Asp82A mutant. *Lane 4*, PepD Asp119A mutant. *Lane 5*, PepD Glu149A mutant. *Lane 6*, PepD Glu150A mutant. *Lane 7*, PepD Asp173A mutant. *Lane 8*, PepD His461A mutant. *Lane 9*, PepD Asp119AGlu150A mutant.

The purified wild-type and mutant PepD proteins were also subjected to the activity assay on L-carnosine as a substrate. The wild-type PepD catalyzed the hydrolysis of L-carnosine under standard conditions as described on 2.9.1, and defined its acitivty as 100%. No apparent activities of PepD H80A, D82A, D119A, E149A, E150A, D173A, and H461A mutants could be detected (Fig. 19), which indicates these residues are involved in the catalysis of PepD on L-carnosine.

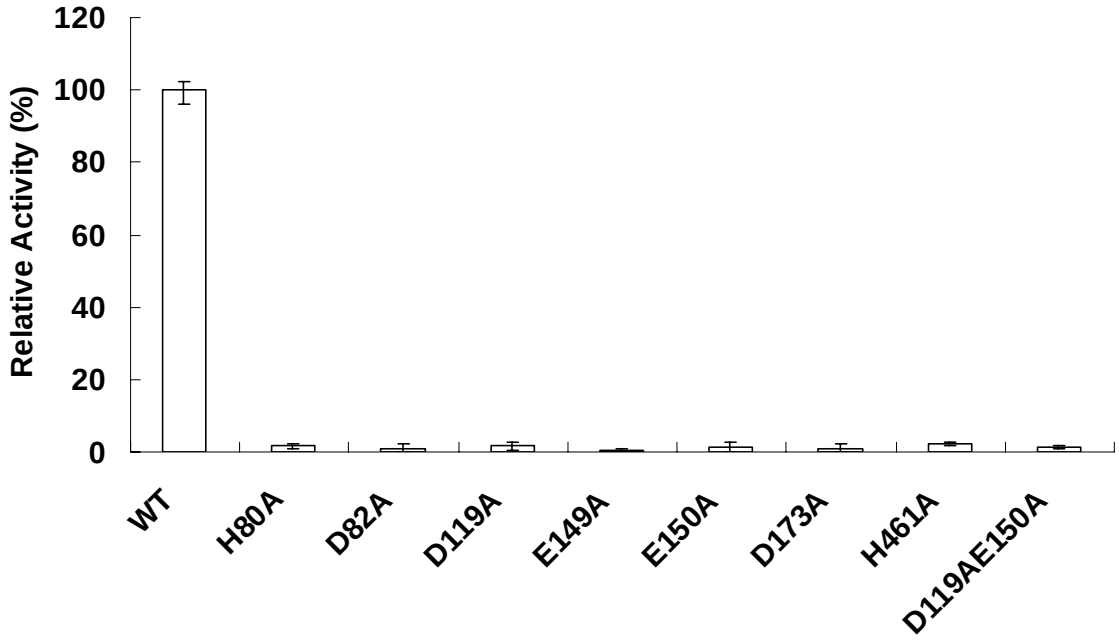

Fig. 19. Enzymatic activities of PepD WT and mutants on L-carnosine.

A potential problem using site-directed mutagenesis techniques is that mutations can cause global conformational changes that inactivate the protein. To verify the mutant effect on PepD conformation, CD spectroscopy was performed on the purified wild-type and mutant proteins. The far-UV CD spectra of PepD mutants are similar to that of the wild-type protein (Fig. 20) (The individual comparison among PepD wild-type, denatured wild-type, and mutant proteins was supplemented at Appendix 7). There are some changes in the 220-200 nm region of the spectra that might result from the single mutant changing the nearby structure of

PepD proteins. However, the overall shape of the wild-type and mutant PepD spectra appear to be similar, the data suggests that the PepD mutants are not grossly misfolded.

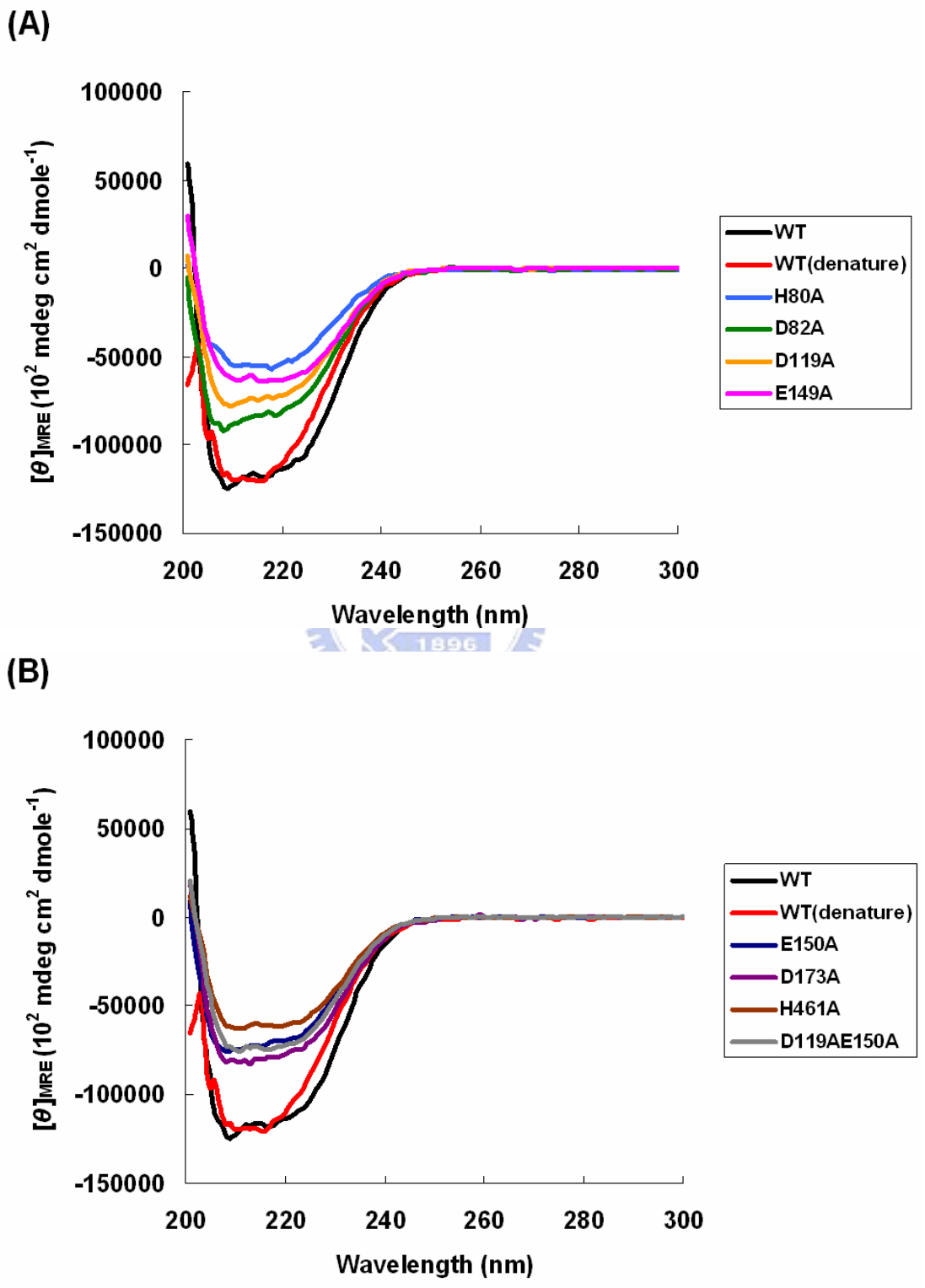

Fig. 20. The CD spectra of *V. alginolyticus* PepD wild-type and mutant proteins.

3.8. Structural Features of PepD

To predict the active site residues of *V. alginolyticus* PepD, the computational analysis was also carried out through homology modeling method. The PepD model was obtained with *L. delbrueckii* PepV as the template. The generated PepD structure is quite similar to PepV structure, though they are very poor in the amino acid sequence identity (9%) (Fig. 21).

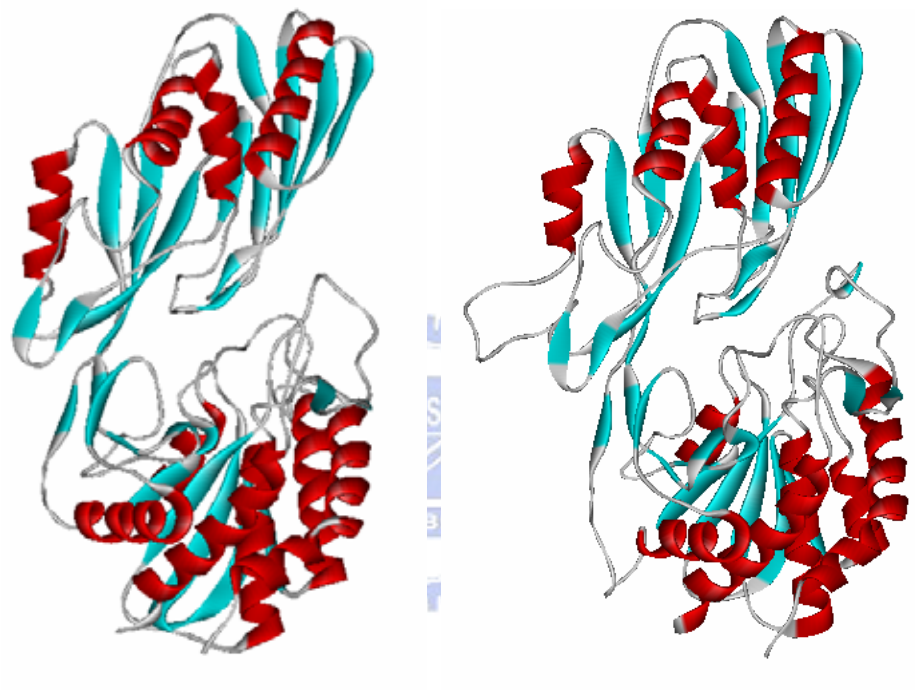

Fig. 21. Three-dimensional ribbon of the crystal structure of PepV (left) and the generated PepD model based on PepV (right).

Surprisingly, the superposition of PepV active site residues with PepD reveals that the predicted active site residues of PepD are almost equivalent to that of PepV (Fig. 22). Only the residue Asp119 of PepD has a notable difference with that of PepV in this model. However, the low sequence indentity between PepD and PepV gives the possibility of mis-simulating at some region of PepD model. Besides, loss of the full activity of PepD D119A mutant indicates that this residue plays an important role in the active site of PepD. In summay, based on the results of sequence alignment, activity assay, and homology modeling,

7 residues are involved in the active site of *V. alginolyticus* PepD including His80, Asp119, Glu150 associated with zinc ion 1, Asp119, Asp173, His461 associated with zinc ion 2, and two catalytic residues Asp82 and Glu149.

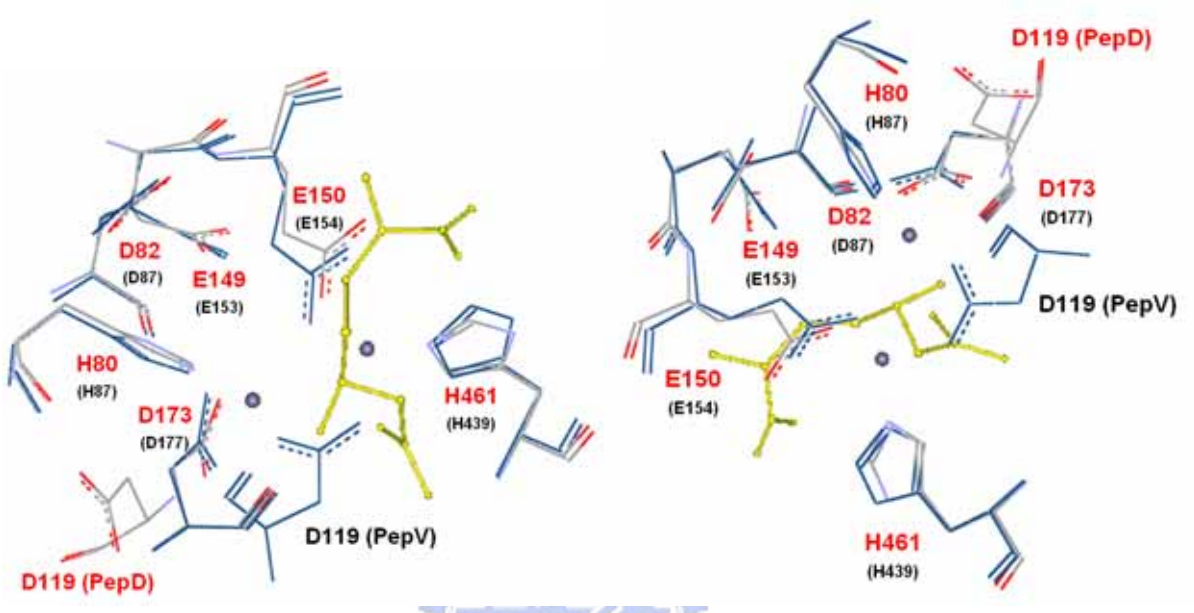

Fig. 22. Stereo view of PepD (light gray) superimposed with the active site of PepV (blue). Residues are numbered (red) according to the PepD sequence. Residues are numbered (black in parenthesis) according to the PepV sequence. The zinc ions and co-crystallized dipeptide analogue inhibitor AspΨ[PO_2CH_2]AlaOH of PepV is depicted in gray and yellow, respectively. The right and left view show only angle in difference.